Investigation of Fano resonance in compound resonant waveguide gratings for optical sensing

Jinhua Hu (胡劲华)[1], Xiuhong Liu (刘秀红)[2,*], Jijun Zhao (赵继军)[1], and Jun Zou (邹 俊)[3]

[1]*The School of Information & Electrical Engineering, Hebei University of Engineering, Handan 056038, China*
[2]*The School of Mathematics & Physics, Hebei University of Engineering, Handan 056038, China*
[3]*College of Science, Zhejiang University of Technology, Hangzhou 310023, China*
**Corresponding author: liuxiuhong@hebeu.edu.cn*

Received September 20, 2016; accepted December 23, 2016; posted online January 22, 2017

An optical sensor is designed to support the Fano effect based on a compound resonant waveguide grating (CRWG). The transmission spectra of the CRWG are investigated by utilizing a theoretical method that combines the temporal coupled mode theory with the eigenmode information of the grating structure. The theoretical results, which are observed to agree closely with those acquired by rigorous coupled-wave analysis, show that the linewidth of the transmission spectrum decreases upon increasing the distance between the grating strips, and the central resonance frequency decreases as the refractive index of the analyte increases. Here, the proposed CRWG structures will find potential uses in optical sensing.

OCIS codes: 050.6624, 130.6010.
doi: 10.3788/COL201715.030502.

High-sensitivity label-free biosensors have been widely used in many fields, for purposes such as medical diagnosis, environmental monitoring, and chemical detection. Label-free biosensors based on resonant structures have been developed rapidly during recent years because they are simple to fabricate and exhibit excellent optical resonance properties[1,2]. Several types of integrated optical devices have been employed as label-free sensors, such as photonic crystals[3], asymmetric plasmonic hexamers[4], and high-contrast-gratings[5]. Recently, resonant waveguide gratings (RWGs) have been demonstrated as an optical sensor by utilizing guided-mode resonance. Different from surface plasmon resonance (SPR) sensors[6] and waveguide mode sensors[7], RWG sensors can be easily integrated without special separate coupling, such as prism coupling or lensed fiber coupling. RWG sensors have drawn much attention. For instance, Wang *et al.* demonstrated a refractive index sensor using an RWG[8], and Zaytseva *et al.* developed a medium-throughput microfluidic biosensor system for whole-cell sensing by employing an RWG structure[9]. Zheng *et al.* demonstrated theoretically and numerically an RWG sensor with a sharp Fano resonance using double-sided dielectric gratings[10]. However, it is difficult to realize the sharp linewidths of the transmission spectra for optical sensing using a single-layer symmetrical RWG. In order to solve this problem, we choose an asymmetrical RWG. The leaky modes of the asymmetrical RWG can be confined in this structure, which allows weak coupling to the sample liquid region.

RWGs are often designed to support Fano resonances using rigorous electromagnetic methods[11–13], which generally originate from the interference between direct and resonance-assisted pathways. Although accurate simulation results have been obtained, most of these methods are mathematically complex and do not provide intuitive explanations of the resonant mechanism of RWG; they are also time consuming. In order to overcome this problem, we previously proposed a theoretical model that can be employed to analyze the transmission spectra of RWG structures with Fano resonances[14]. This model combines the temporal coupled-mode theory (TCMT) with the grating structure's eigenmode information and assumes the RWG is a single-mode structure. However, most RWGs that are employed in optical sensing contain integrated bottom layers and asymmetrical structures. To elucidate the Fano resonance mechanism of asymmetric RWGs with bottom layers intuitively and to enable the design of high-performance sensors, we herein propose an asymmetric compound resonant waveguide grating (CRWG) with a Fano resonance, which contains the different widths of compound gratings in a unit cell. In addition, we present the results of the theoretical analysis of this CRWG, which were obtained using a theoretical method. These results may simplify the design of Fano-resonant grating structures for a variety of optical sensing applications.

Figure 1 shows a schematic diagram of the proposed CRWG-based optical sensor structure, which contains two separate grating strips in each period and is covered by a sample liquid with a refractive index of n_{cl}. The refractive indices of the silicon grating layer and the silica substrate layer are $n_{\mathrm{Si}} = 3.45$ and $n_{\mathrm{SiO_2}} = 1.48$, respectively. The CRWG is considered to be infinite in the y-direction and periodic in the x-direction. The parameters of the proposed sensor are as follows: the compound grating period is P, the widths of the two grating strips in each period are W_1 and W_2, the interspacing between the two grating strips in each period is L_1, and the thickness of the grating is d. In our proposed model, the CRWG is viewed as a single-mode resonator. The grating structure's eigenmode information is determined by performing a

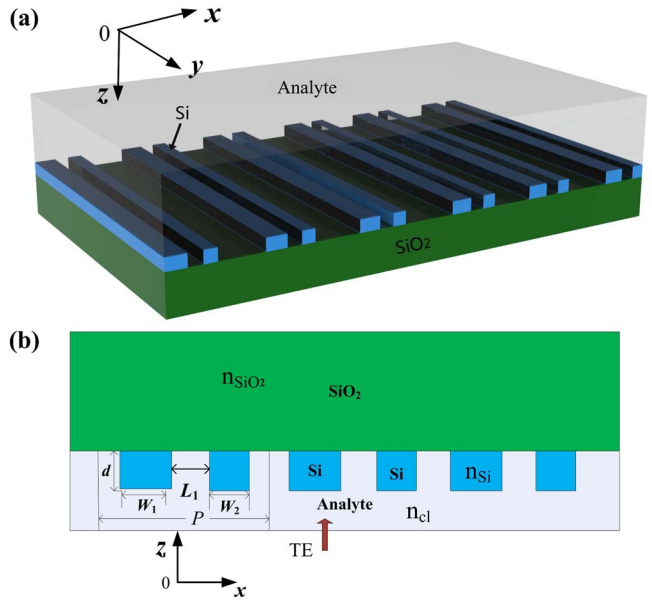

Fig. 1. Schematic of the CRWG sensor.

finite element method (FEM) simulation, and the lineshape function is then calculated using TCMT.

In this method, a single period of the CRWG structure is defined as a unit cell, and the silicon and silica can be considered lossless. Floquet periodic boundary conditions are applied to the lateral boundaries, and scattering boundary conditions are applied to the upper and lower boundaries. The CRWG eigenmode information is obtained using the FEM[14,15]. Next, the CRWG structure is considered to be a uniform slab, and its amplitude reflection coefficient r and transmission coefficient t are both calculated. Since the CRWG structure is an asymmetrical single-mode resonator due to its silica substrate, a small correction is applied to the eigenvalues N, which have the form $N = N_{\text{real}} - \text{i} * N_{\text{imag}}$, where N_{real} and N_{imag} are the real and imaginary parts of N, respectively. Then, the transmission spectrum of the CRWG can be calculated using[14,16]

$$T = 1 - \frac{r^2(\omega - N_{\text{real}}) + t^2 N_{\text{imag}} - 2rt(\omega - N_{\text{real}})N_{\text{imag}}}{(\omega - N_{\text{real}})^2 + N_{\text{imag}}^2}, \tag{1}$$

where the central resonance frequency ω_0 and total radiative quality factor q_0 of the CRWG structure can be obtained using[17]

$$\begin{cases} \omega_0 = N_{\text{real}} \\ q_0 = N_{\text{real}}/2N_{\text{imag}} \end{cases}. \tag{2}$$

Thus, the lineshape function of the CRWG can be predicted directly. Furthermore, the sensitivity S and figure of merit (FOM) of the CRWG sensor can be calculated by varying n_{cl}. To check the validity of this theoretical model, we compared its predictions with a rigorous coupled-wave analysis (RCWA) simulation of the Fano resonance in the CRWG. We chose a unit cell of the CRWG, where Floquet periodic boundary conditions are applied for the lateral boundaries and scattering boundary conditions are applied for the upper and lower boundaries. The structural parameters are $L_1 = 206$ nm, $W_1 = 302$ nm, $W_2 = 202$ nm, $P = 980$ nm, and $d = 160$ nm. The eigenvalues of the TE eigenmodes of the CRWG structure corresponding to different n_{cl} were calculated using the FEM and are listed in Table 1. The eigenvalues clearly vary with n_{cl} and indicate that ω_0 decreases with increasing n_{cl}. In other words, the resonant peak is red-shifted as n_{cl} increases from 1.330 to 1.334.

We determined the resonant wavelengths and linewidths of the Fano resonances from the transmission spectra of the CRWG sensor that were obtained using Eq. (1) after correcting the values of N. These theoretical spectra as well as the RCWA simulation results are presented in Fig. 2, which shows that the calculated spectra agree well with the simulation results.

Next, we calculated S using the definition

$$S = \Delta\lambda_{\text{res}}/\Delta n_{\text{cl}}, \tag{3}$$

where $\Delta\lambda_{\text{res}}$ is the resonance wavelength shift, and Δn_{cl} is the change in n_{cl}. We obtained the CRWG sensor's

Table 1. Eigenvalues of TE Eigenmodes Corresponding to Different Refractive Indices

Refractive Index n_{cl}	Eeigenvalue N
1.330	$1.20826 \times 10^{15} - 1.36527 \times 10^{12}i$
1.332	$1.20791 \times 10^{15} - 1.36523 \times 10^{12}i$
1.334	$1.20734 \times 10^{15} - 1.36514 \times 10^{12}i$

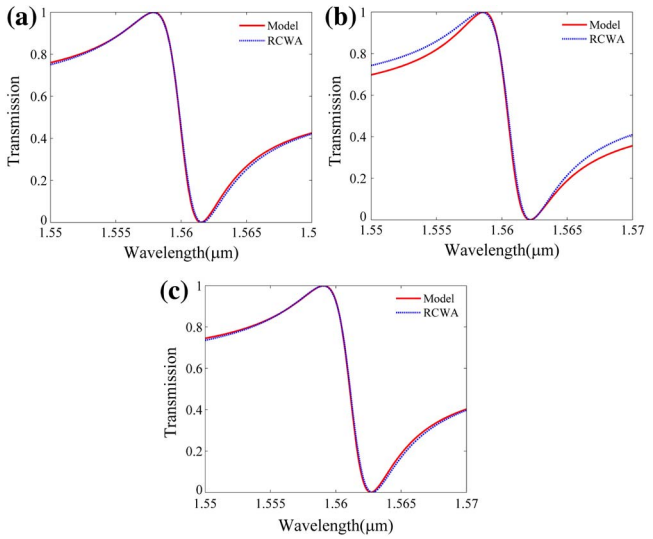

Fig. 2. CRWG transmission spectra for TE eigenmodes corresponding to (a) $n_{\text{cl}} = 1.330$, (b) $n_{\text{cl}} = 1.332$, and (c) $n_{\text{cl}} = 1.334$.

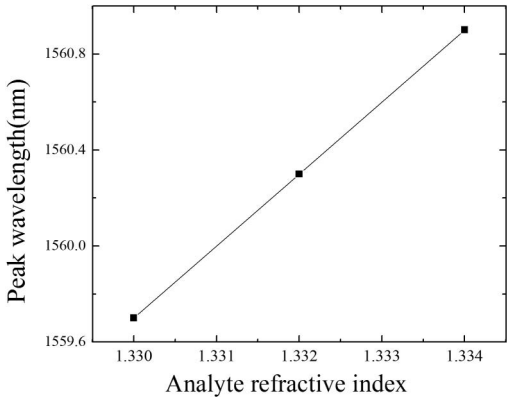

Fig. 3. CRWG resonance peak wavelength versus n_{cl}.

resonant peak wavelengths, which are plotted against n_{cl} in Fig. 3, using the corrected values of N. For the proposed CRWG sensor, S was found to be 300 nm/RIU.

To evaluate the bio-sensing performance of the CRWG, we then calculated FOM using

$$\mathrm{FOM} = S/\Delta\lambda, \tag{4}$$

where $\Delta\lambda$ is the full width at half-maximum (FWHM). This equation indicates that the FOM will increase as the FWHM of the spectrum decreases. Thus, it is important to determine an effective method of controlling the Fano resonance linewidths of RWG structures. Several research groups have examined this issue[18–20]. In this study, we investigated the dependence of the FWHM on L_1 by comparing the theoretic model results with the RCWA simulated results, which are presented in Fig. 4. We demonstrate that they fit very well. Interestingly, the FWHM decreases with the increase of L_1. Thus, the sharp Fano-type lineshape of the transmission spectra is exhibited in the proposed CWRG structure. Our theoretical model, which directly relates the Fano resonance linewidth to the parameters of the CRWG structure, should easily understand the physical concepts of Fano resonances.

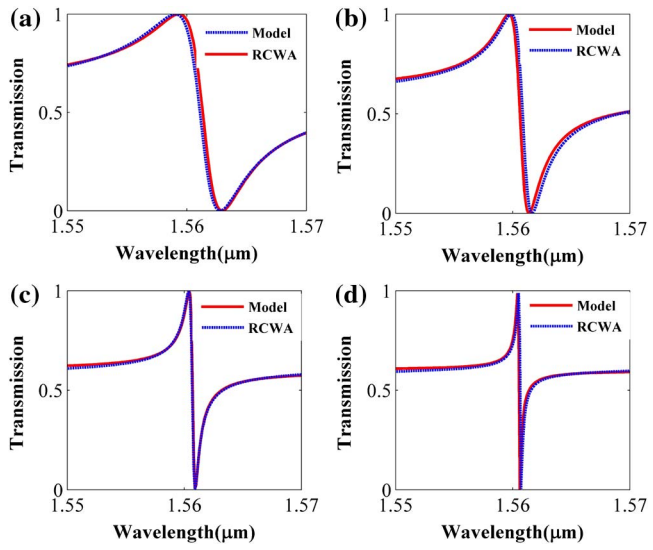

Fig. 4. CRWG transmission spectra for TE polarization and different L_1, $n_{cl} = 1.332$, $W_1 = 302$ nm, $W_2 = 202$ nm, $P = 980$ nm, and $d = 160$ nm. (a) $L_1 = 206$ nm, (b) $L_1 = 216$ nm, (c) $L_1 = 226$ nm, and (d) $L_1 = 231$ nm.

To gain further insight into the physical origin of the differences between the Fano resonance linewidths of the CRWGs, we used the proposed model to determine N for the TE eigenmode corresponding to each value of L_1. The results, shown in Table 2, indicate that N_{real} is insensitive to changes in L_1, while N_{imag} varies. Consequently, according to Eq. (2), ω_0 remains relatively constant when L_1 changes, while q_0 is significantly enhanced as L_1 increases. Physically, the interspacing of the two grating strips is relatively large (almost comparable to the width of single grating strip), and weak coupling exists between compound gratings. The resonant wavelength is mainly determinate by two grating strips in the unit cell and shows little dependence on the interspacing L_1. These findings indicate that the Fano resonance linewidth of a CRWG can be controlled by adjusting L_1.

Finally, we used the proposed method to calculate the transmission spectrum of the CRWG structure when it was covered with analyte liquids with different n_{cl}, and the other structural parameters were as follows: $L_1 = 231$ nm, $P = 980$ nm, $d = 160$ nm, $W_1 = 302$ nm, and $W_2 = 202$ nm. The obtained spectra, which are depicted in Fig. 5, reveal that the Fano resonance peak shifts

Table 2. Eigenvalues of TE Eigenmodes for Different L_1

L_1 (nm)	Eigenvalue N
206	$1.20791 \times 10^{15} - 1.36523 \times 10^{12} i$
216	$1.20545 \times 10^{15} - 6.44717 \times 10^{11} i$
226	$1.20554 \times 10^{15} - 1.93664 \times 10^{11} i$
231	$1.20557 \times 10^{15} - 6.70643 \times 10^{10} i$

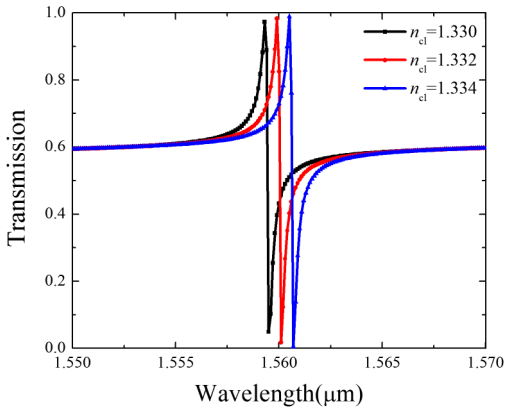

Fig. 5. CRWG transmission spectra for TE polarization with different n_{cl}, $L_1 = 231$ nm, $P = 980$ nm, $d = 160$ nm, $W_1 = 302$ nm, and $W_2 = 202$ nm.

as n_{cl} changes. Based on these results, S and FOM were determined to be 350 nm/RIU and 437.5, respectively.

We investigate the Fano resonance characteristics of a CRWG structure, which can be employed as an optical sensor, using an improved theoretical model. We study the linewidths of the CRWG structure's transmission spectra by changing the grating parameters to obtain different resonance eigenmodes. The lineshapes of the Fano resonance spectra are found to be dependent upon the eigenmodes, which are determined by the CRWG structure. The proposed CRWG structure can easily achieve sharp lineshapes of the Fano resonance. The resonant wavelength of CRWG is very sensitive to small changes of the analyte index. Therefore, the designed CRWG will have potential applications in optical sensing. Furthermore, the proposed theoretical model provides a convenient method of investigating the Fano resonance characteristics of high-performance optical sensors.

This work was supported by the Scientific Research Projects of the Department of Education of Hebei Province (Nos. QN2014134 and QN2016090), the Natural Science Foundation of Hebei Province (No. A2015402035), and the National Natural Science Foundation of China (NSFC) (No. 61605172).

References

1. P. Dumais, C. L. Callender, J. P. Noad, and C. J. Ledderhof, Opt. Express **16**, 18164 (2008).
2. X. Jiang, J. Ye, J. Zou, M. Li, and J.-J. He, Opt. Lett. **38**, 1349 (2013).
3. M. Huang, A. Yanik, T. Chang, and H. Altug, Opt. Express **17**, 24224 (2009).
4. H. D. Deng, X. Y. Chen, Y. Xu, and A. E. Miroshnichenko, Nanoscale **7**, 20405 (2015).
5. A. Liu, W. H. E. Hofmann, and D. H. Bimberg, IEEE J. Quantum Electron. **51**, 1 (2015).
6. G. Lan, S. Liu, X. Zhang, Y. Wang, and Y. Song, Chin. Opt. Lett. **14**, 022401 (2016).
7. B. Wei, C. Zhao, G. Wang, T. Dai, J. Yang, K. Zhou, and Y. Li, Chin. Opt. Lett. **14**, 031301 (2016).
8. J. J. Wang, L. Chen, S. Kwan, F. Liu, and X. Deng, J. Vac. Sci. Technol. B **23**, 3006 (2005).
9. N. Zaytseva, W. Miller, V. Goral, and Y. Fang, Appl. Phys. Lett. **98**, 163703 (2011).
10. G. Zheng, L. Zhao, L. Qian, F. Xian, and L. Xu, Opt. Commun. **358**, 140 (2016).
11. M. G. Moharam, D. A. Pommet, E. B. Grann, and T. K. Gaylord, J. Opt. Soc. Am. A **12**, 1077 (1995).
12. M. G. Moharam, E. B. Grann, D. A. Pommet, and T. K. Gaylord, J. Opt. Soc. Am. A **12**, 1068 (1995).
13. A. Taflove and S. C. Hagness, *Computational Electrodynamics: The Finite-Difference Time-Domain Method*, 3rd Revised Edition (Artech House Publishers, 2005).
14. J. H. Hu, Y. Q. Huang, X. M. Ren, X. F. Duan, Y. H. Li, Q. Wang, X. Zhang, and J. Wang, Chin. Phys. Lett. **31**, 064205 (2014).
15. W. E. I. Sha, L. L. Meng, W. C. Choy, and W. C. Chew, Opt. Lett. **39**, 158 (2014).
16. S. Fan, W. Suh, and J. D. Joannopoulos, J. Opt. Soc. Am. A **20**, 569 (2003).
17. L. Huang, Y. Yu, and L. Cao, Nano Lett. **13**, 3559 (2013).
18. W. X. Liu, Y. H. Li, H. T. Jiang, Z. Q. Lai, and H. Chen, Opt. Lett. **38**, 163 (2013).
19. M. Song, H. Yu, C. Wang, N. Yao, M. Pu, J. Luo, Z. Zhang, and X. Luo, Opt. Express **23**, 2895 (2015).
20. D. Zhang, L. Yuan, J. Chen, S. Zhuang, and H. He, Chin. Opt. Lett. **6**, 776 (2008).